Progress In Electromagnetics Research C, Vol. 110, 15–26, 2021

Analysis of a Nonlinear Magnetic Coupling Wireless Power Transfer System

Meng Wang, Li Ren, Yanyan Shi*, Weina Liu*, and Haoran Wang

Abstract—In near-field energy transmission, it has been proved that magnetic coupling wireless power transfer (MC-WPT) is a promising energy transmission method. Traditionally, the MC-WPT system is established based on a linear resonant circuit. Recently, it has been reported that nonlinear MC-WPT system shows more advantages. However, nonlinear characteristics of the nonlinear MC-WPT system are not fully recovered. In this paper, a nonlinear MC-WPT system which can be described by Duffing equation is presented. The mathematical model of the equivalent circuit is developed. The related nonlinear characteristics under the impact of driving force are investigated. It is found that the driving force has a direct impact on the system performance. The operation of the nonlinear MC-WPT system varies from periodic sinusoidal state to periodic non-sinusoidal state even to chaotic state when the driving force increases. It should be mentioned that the chaotic state should be avoided. Generally, the MC-WPT system should be operated in periodic sinusoidal state which only covers a small range of driving force. For the system operated in periodic non-sinusoidal state, a waveform correcting circuit is designed. The simulated and experimental results show that the restriction of the driving force on the operation of the system is eliminated with a waveform correcting circuit added. It is possible for the nonlinear MC-WPT system to be operated in a much wider range.

1. INTRODUCTION

Traditionally, electric power is delivered by wired connection which inevitably induces power loss. Also, the transfer performance is affected by aging of line. Therefore, a more efficient and convenient method is urgently required for power transfer. In recent years, wireless power transfer (WPT) has received considerable attention [1–5]. With this technique, the power can be delivered to load without mechanical contact [6–8]. Generally, the WPT technique is categorized into magnetic inductive WPT and magnetic coupling WPT (MC-WPT). Due to the advantage of mid-range power transfer, MC-WPT is preferred [9–14]. Nowadays, MC-WPT has been used in a variety of applications such as the powering of electronic devices, medical implanted devices, and electric vehicles [15–19].

The configuration of a typical two-coil MC-WPT system is shown in Fig. 1. The transmitting coil is connected to a power source via a compensation capacitor. Through the exchange of electromagnetic energy, the power is delivered to the receiving coil from which the load can be powered. It should be noted that a compensation capacitor is also required in the receiving side of the MC-WPT system. The two capacitors are used to make the loops resonate at a specific frequency.

Due to its simple configuration, two-coil MC-WPT system has been commonly applied to wireless power transfer [20–24]. However, the transfer performance is affected by transfer distance, magnetic coupling between coils, and coil parameters. To deal with the problems, various methods such as impedance matching, adding materials with high permeability, and using high-Q resonant coils are proposed to enhance the transfer performance. In [25], a novel serial/parallel capacitor matrix is

Received 31 December 2020, Accepted 5 February 2021, Scheduled 16 February 2021
* Corresponding author: Yanyan Shi (yyshi113@hotmail.com), Weina Liu (weinaliu926@163.com).
The authors are with the College of Electronic and Electrical Engineering, Henan Normal University, Xinxiang, Henan 453007, China.

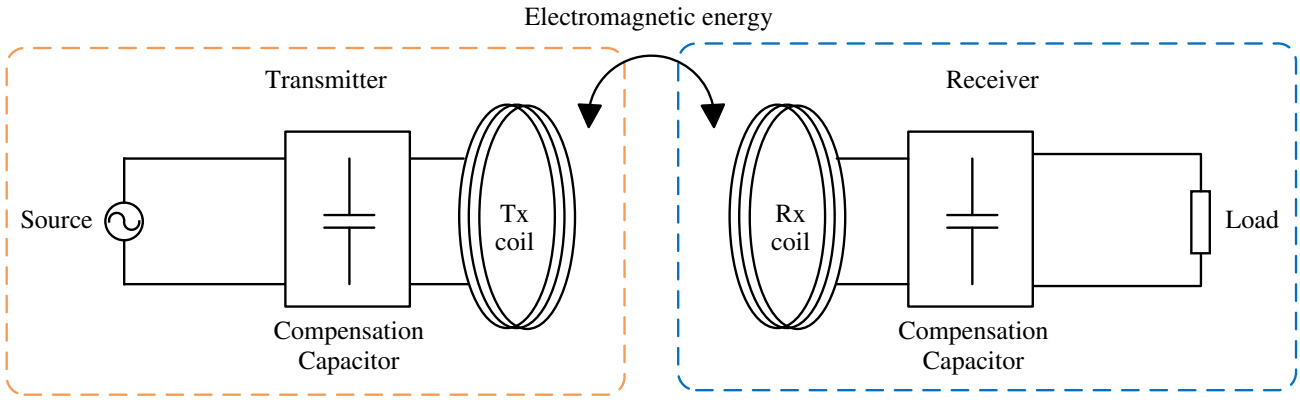

Figure 1. A typical magnetic coupling wireless power transfer system.

applied in the transmitter with which the impedance can be automatically matched with the optimal impedance-matching point when the transfer distance varies. In [26], on the assumption of decreasing demagnetizing factor and improving mutual inductance, a two-coil MC-WPT system with a novel ferrite core introducing inside the coils is proposed, and the transfer performance is greatly enhanced. In addition, the MC-WPT system with a high-Q value is preferred for its excellent performance in power transfer [27, 28]. It should be noted that all these methods are presented based on linear resonant circuit. Generally, a linear MC-WPT system is characterized with a narrow bandwidth. This would reduce system tolerance to deviation of resonant frequency which is usually inevitable in actual applications. To cope with the problem, a four-coil MC-WPT system featured with broadband performance is designed in [29]. Recently, nonlinear MC-WPT systems have received considerable attention. In [30], by adopting equivalent small parameter method, a nonlinear mathematical model is established for the WPT system with a class-E inverter. The results demonstrate that sufficient accuracy is realized when harmonics with higher-order are considered. In [31], a robust MC-WPT system which is based on a parity-time-symmetric circuit is presented. It is advantageous in remaining high transfer efficiency over a wide transfer distance. As well known, the mutual coupling between transmitting and receiving coils varies due to the change of transfer distance. To reduce sensitivity, a novel MC-WPT system based on a nonlinear resonant circuit is proposed in [32]. It is found that the transfer efficiency is still kept at high value when the distance between coils varies.

There are a variety of configurations for linear WPT systems such as series-series structure, series-parallel structure, parallel-series structure, and parallel-parallel structure. Among these structures, series-series configuration has been widely applied to wireless power transfer. In this work, a series-series compensated nonlinear WPT system is mainly discussed. Generally, an MC-WPT system is supposed to be operated in periodic sinusoidal state. In this paper, a nonlinear MC-WPT system which can be operated in periodic non-sinusoidal state is investigated. Section 2 presents the equivalent model of the nonlinear MC-WPT system. Also, the mathematical description is given. In Section 3, the nonlinear characteristics of the nonlinear WPT system are studied, based on which the nonlinear MC-WPT system with an additional waveform correcting circuit is designed. In Section 4, the experimental validation is performed. Finally, conclusions are drawn in Section 5.

2. MODELING OF A NONLINEAR MC-WPT SYSTEM

For the MC-WPT system based on a linear resonant circuit, all the electric components are linear. A nonlinear system is established if a nonlinear component is introduced. Mathematically, the general form of Duffing equation is described by [33]

$$\frac{d^2x}{dt^2} + 2\xi\frac{dx}{dt} + w_0^2 x + \delta x^3 = F_a \cos(\Omega t) \tag{1}$$

where x, t, ξ, w_0, δ, F_a, and Ω respectively denote displacement, time, damping ratio, oscillation frequency, cubic stiffness, driving amplitude, and excitation frequency.

By introducing a nonlinear capacitor, a two-coil series-series MC-WPT system based on the nonlinear Duffing equation is developed in Fig. 2. In Fig. 2(a), R_s and R_l are respectively the resistance of the source v_s and the load; L_1 and L_2 are respectively the inductance of transmitting coil and receiving coil; C_1 is the capacitance used for resonance of the transmitter while C_2 is the nonlinear capacitor in the receiver; M is mutual inductance between coils. Fig. 2(b) depicts the equivalent circuit of Fig. 2(a), in which v_e and R_e are respectively the equivalent power and reflected resistance when the transmitter is operated in resonant state. It should be noted that v_e is determined by v_s and M while R_e is mainly determined by M for an MC-WPT system operated in resonant state.

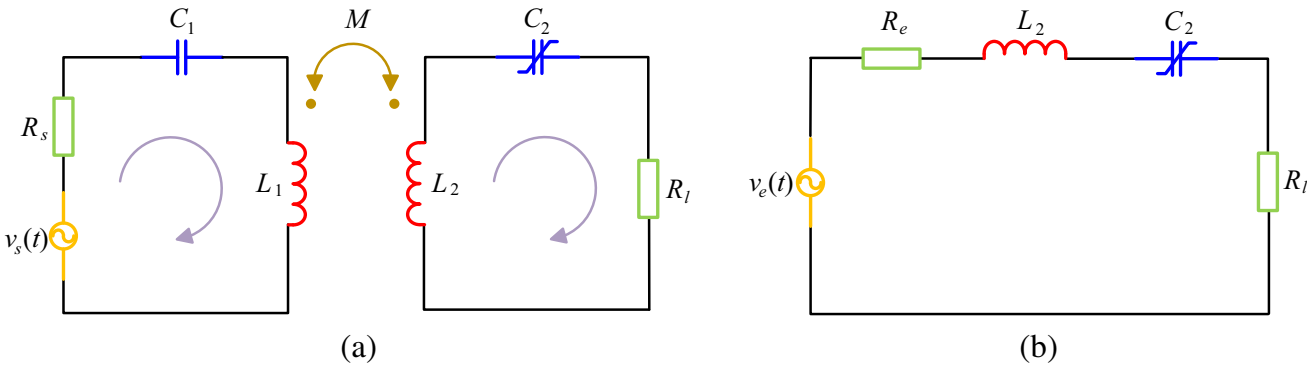

Figure 2. A nonlinear MC-WPT system. (a) Circuit model based nonlinear resonance. (b) Equivalent circuit.

Based on Kirchhoff voltage law (KVL), the dynamic behavior of the equivalent MC-WPT system can be described by:

$$L_2\frac{d^2q_c(t)}{dt^2}+R\frac{dq_c(t)}{dt}+v_c(t)=v_e(t) \tag{2}$$

where $v_e=V_{E*}\cos(\omega t)$, ω is the excitation frequency, $R=R_e+R_l$, v_c the voltage across the nonlinear capacitor, and q_c the charge stored in the nonlinear capacitor.

For a nonlinear capacitor with symmetric relationship between capacitance and voltage, the voltage v_c across the capacitor can be expressed by the charge q_c as [34]

$$v_c(t)=\frac{1}{b_1}q_c(t)+\frac{1}{b_3}q_c^3(t) \tag{3}$$

where b_1 is the linear coefficient, and b_3 is the nonlinear coefficient.

Substituting Eq. (3) into Eq. (2) results in:

$$\frac{d^2q_c}{dt^2}+\frac{R}{L_2}\cdot\frac{dq_c}{dt}+\frac{1}{L_2b_1}q_c+\frac{1}{L_2b_3}q_c^3=\frac{V_E}{L_2}\cos(\omega t) \tag{4}$$

Comparing Eq. (4) with Eq. (1), it can be observed that the mathematical model of Fig. 2(b) is a Duffing equation. For simplicity, Eq. (4) can be rewritten as:

$$\frac{d^2q_c}{dt^2}+k\frac{dq_c}{dt}+w_1^2q_c+\alpha q_c^3=\mu\cos(\omega t) \tag{5}$$

in which

$$k=\frac{R}{L_2},\ w_1^2=\frac{1}{L_2b_1},\ \alpha=\frac{1}{L_2b_3},\ \mu=\frac{V_E}{L_2}$$

In order to analyze the nonlinear MC-WPT system with method of multiple scales, a dimensionless expression of Eq. (5) is required. With a dimensionless variable $\tau=w_1t$ introduced, Eq. (5) is transformed into

$$\frac{d^2q_c}{d\tau^2}+k'\frac{dq_c}{d\tau}+q_c+\alpha' q_c^3=\mu'\cos(\Omega'\tau) \tag{6}$$

in which

$$k^{'} = \frac{k}{w_1},\ \alpha^{'} = \frac{\alpha}{w_1^2},\ \mu^{'} = \frac{\mu}{w_1^2},\ \Omega^{'} = \frac{\omega}{w_1}$$

In addition, a dimensionless variable $Q = \sqrt{\alpha^{'}} q_c$ is introduced. Eq. (6) is finally converted into

$$\frac{d^2Q}{d\tau^2} + k^{'}\frac{dQ}{d\tau} + Q + Q^3 = F\cos(\Omega^{'}\tau) \tag{7}$$

in which

$$F = \sqrt{\alpha^{'}} \cdot \mu^{'}.$$

To determine the analytical approximation of Eq. (7), perturbation analysis is generally applied. A small parameter ε $(0 < \varepsilon < 1)$ is introduced. In this work, the forced oscillation at the primary resonance is considered. To describe the approximation of excitation frequency to system natural frequency, a detuning parameter σ is defined, and Eq. (7) is rewritten as:

$$\frac{d^2Q}{d\tau^2} + Q + \varepsilon\left(\varsigma\frac{dQ}{d\tau} + \gamma Q^3\right) = \varepsilon F^{'}\cos((1+\varepsilon\sigma)\tau) \tag{8}$$

in which

$$\varsigma = \frac{k^{'}}{\varepsilon},\ \gamma = \frac{1}{\varepsilon},\ F^{'} = \frac{F}{\varepsilon}$$

It is difficult to obtain the exact analytical solution of Eq. (8). However, by introducing multiple timescales, the approximate analytical solution can be calculated with the method of multiple scales [35]. According to this method, a fast timescale T_0 and a slow timescale T_1 are respectively defined as:

$$T_0 = \tau,\ T_1 = \varepsilon\tau \tag{9}$$

Then, the derivatives with respect to τ are transformed into:

$$\begin{cases} \dfrac{d}{d\tau} = \dfrac{\partial}{\partial T_0} + \varepsilon\dfrac{\partial}{\partial T_1} = D_0 + \varepsilon D_1 \\ \dfrac{d^2}{d\tau^2} = D_0^2 + 2\varepsilon D_0 D_1 + \varepsilon^2(D_1^2 + 2D_0D_1) \end{cases} \tag{10}$$

where $D_n = \frac{\partial}{\partial T_n}$ $(n = 0,\ 1)$.

Suppose that the solution of Eq. (8) is approximated by:

$$Q(\tau;\varepsilon) = Q_0(T_0, T_1) + \varepsilon Q_1(T_0, T_1) \tag{11}$$

Substituting Eqs. (9)$\sim$(11) into Eq. (8), it can be obtained that

$$\begin{cases} D_0^2Q_0 + Q_0 = 0 \\ D_0^2Q_1 + Q_1 = -2D_0D_1Q_0 - \varsigma D_0Q_0 - \gamma Q_0^3 + F^{'}\cos(T_0 + \sigma T_1) \end{cases} \tag{12}$$

For the first equation in Eq. (12), the solution can be expressed as:

$$Q_0(T_0, T_1) = A(T_1)e^{jT_0} + A^*(T_1)e^{-jT_0} \tag{13}$$

where $A(T_1)$ is a complex valued amplitude function, and $*$ is a complex conjugate of the quantity.

Substituting Eq. (13) into the second equation of Eq. (12), it can be found that:

$$D_0^2Q_1 + Q_1 = \left[-j\left(2\frac{dA}{dT_1} + \varsigma A\right)e^{jT_0} - 3\gamma A^2A^*e^{jT_0} + \frac{F^{'}}{2}e^{jT_0}e^{j\sigma T_1}\right] + cc + NET \tag{14}$$

where cc indicates the complex conjugate of the term in [ ], and NET stands for the terms that will not produce secular terms.

To obtain a bounded solution of Eq. (14), the secular term should be eliminated that is:

$$-j\left(2\frac{dA}{dT_1} + \varsigma A\right)e^{jT_0} - 3\gamma A^2A^*e^{jT_0} + \frac{F^{'}}{2}e^{jT_0}e^{j\sigma T_1} = 0 \tag{15}$$

The complex amplitude $A(T_1)$ in Eq. (15) can be expressed as:

$$A(T_1) = \frac{1}{2}a(T_1)e^{j\beta(T_1)} \tag{16}$$

where $a(T_1)$ and $\beta(T_1)$ are respectively the real-valued amplitude and angle.

Substituting Eq. (16) into Eq. (15), it results in that

$$j\frac{da}{dT_1} - a\frac{d\beta}{dT_1} + j\varsigma a + \frac{3}{8}\gamma a^3 - \frac{1}{2}F'\cos(\sigma T_1 - \beta) - \frac{1}{2}jF'\sin(\sigma T_1 - \beta) = 0 \tag{17}$$

By separating the real and imaginary parts of Eq. (17), it can be obtained that

$$\begin{cases} \dfrac{da}{dT_1} = -\varsigma a - \dfrac{F^{'}}{2}\sin\phi \\ a\dfrac{d\phi}{dT_1} = -\left(\sigma a - \dfrac{3}{8}\gamma a^3 + \dfrac{F^{'}}{2}\cos\phi\right) \end{cases} \tag{18}$$

in which

$$\phi(T_1) = -(\sigma T_1 - \beta)$$

It should be noted that $\frac{da}{dT_1}$ and $\frac{d\phi}{dT_1}$ in Eq. (18) is generally set to 0 for steady-state solution. Then it can be obtained that:

$$F'^2 = 4a^2\left(\varsigma^2 + \left(\sigma - \frac{3}{8}\gamma a^2\right)^2\right) \tag{19}$$

where $F^{'}$ and a are referred to as driving force and amplitude.

For a fixed MC-WPT system, it can be found from the above analysis that $F^{'}$ is related to the powering excitation amplitude linked to transmitting coil and the mutual inductance between coils. Besides, the mutual inductance would also affect the parameter ς. The variation of transfer distance would cause change of mutual inductance. In this work, the transfer distance is fixed, and we mainly focus on the impact of driving force which reflects powering excitation amplitude. However, it should be mentioned that the theoretical analysis is also applicable to the system operated at other transfer distance.

3. NONLINEAR CHARACTERISTICS ANALYSIS

From Eq. (19), it can be found that the driving force has an impact on the amplitude. The variation of the amplitude a against the driving force when $\varsigma = 0.1, \varepsilon = 0.8$ is shown in Fig. 3, where ς is a system

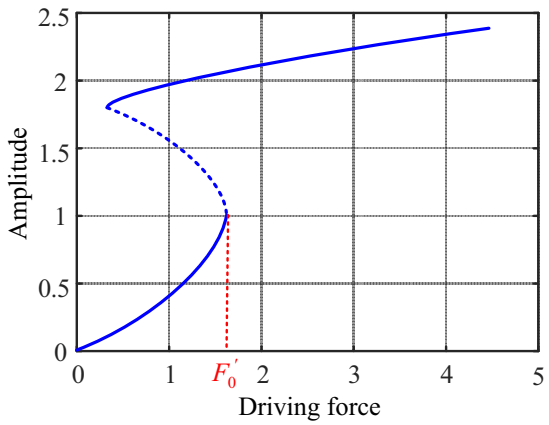

Figure 3. The variation of amplitude against driving force.

related parameter, and ε is a small disturbance parameter. With the quasi-static increase of the driving force, it can be observed from Fig. 3 that the dimensionless amplitude moves on the lower equilibrium branch at first. Then a region with three coexisting solutions is observed where the solid line and dashed line correspond to stable and unstable branches, respectively. Depending on the initial condition, the steady-state solution of the system converges to one of two stable solutions. Jump behavior occurs at the driving force $F_0^{'} = 1.6$.

According to Eq. (7), the simulated phase locus and transient response when $F^{'} = 0.25$ and $F^{'} = 2.5$ are compared in Fig. 4. From Fig. 4(a) and Fig. 4(c), it can be found that the system is operated in periodic state. However, by comparing Fig. 4(b) with Fig. 4(d), the transient responses are different for the driving force smaller and larger than the jump point. The nonlinear MC-WPT system is operated in periodic sinusoidal state when $F^{'} = 0.25$ and in non-sinusoidal state when $F^{'} = 2.5$. As $Q = \sqrt{\alpha'} q_c$ and $\tau = w_1 t$, $\frac{dQ}{d\tau}$ can be regarded as an indicator of the current. Distortion is observed when the driving force is larger. It should be noted that the nonlinear system is operated in periodic sinusoidal state merely in a small range.

Based on Eq. (7), the bifurcation diagram is depicted in Fig. 5. It can be observed from Fig. 5(a) that the nonlinear MC-WPT system is operated in periodic state when the driving force is smaller than 40. Nevertheless, the nonlinear MC-WPT system is in the chaotic state once the driving force is larger than 40. The related phase locus and transient response of the nonlinear system when $F^{'} = 50$ are respectively given in Fig. 5(b) and Fig. 5(c). Comparing Fig. 5 with Fig. 4, obvious chaos state is observed which should be avoided. To conclude, the nonlinear system is operated in the periodic state

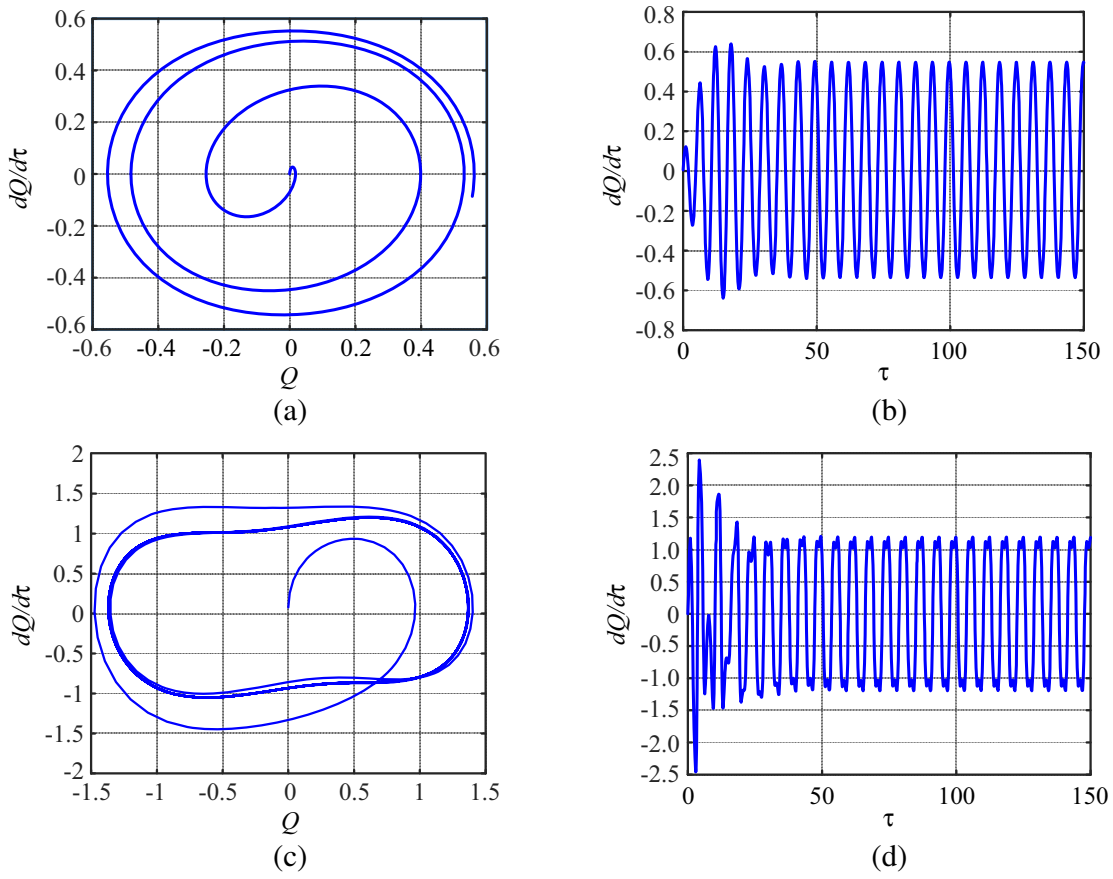

Figure 4. Nonlinear characteristics of the equivalent WPT system. (a) Phase diagram when $F^{'} = 0.25$. (b) Transient response when $F^{'} = 0.25$. (c) Phase diagram when $F^{'} = 2.5$. (d) Transient response when $F^{'} = 2.5$.

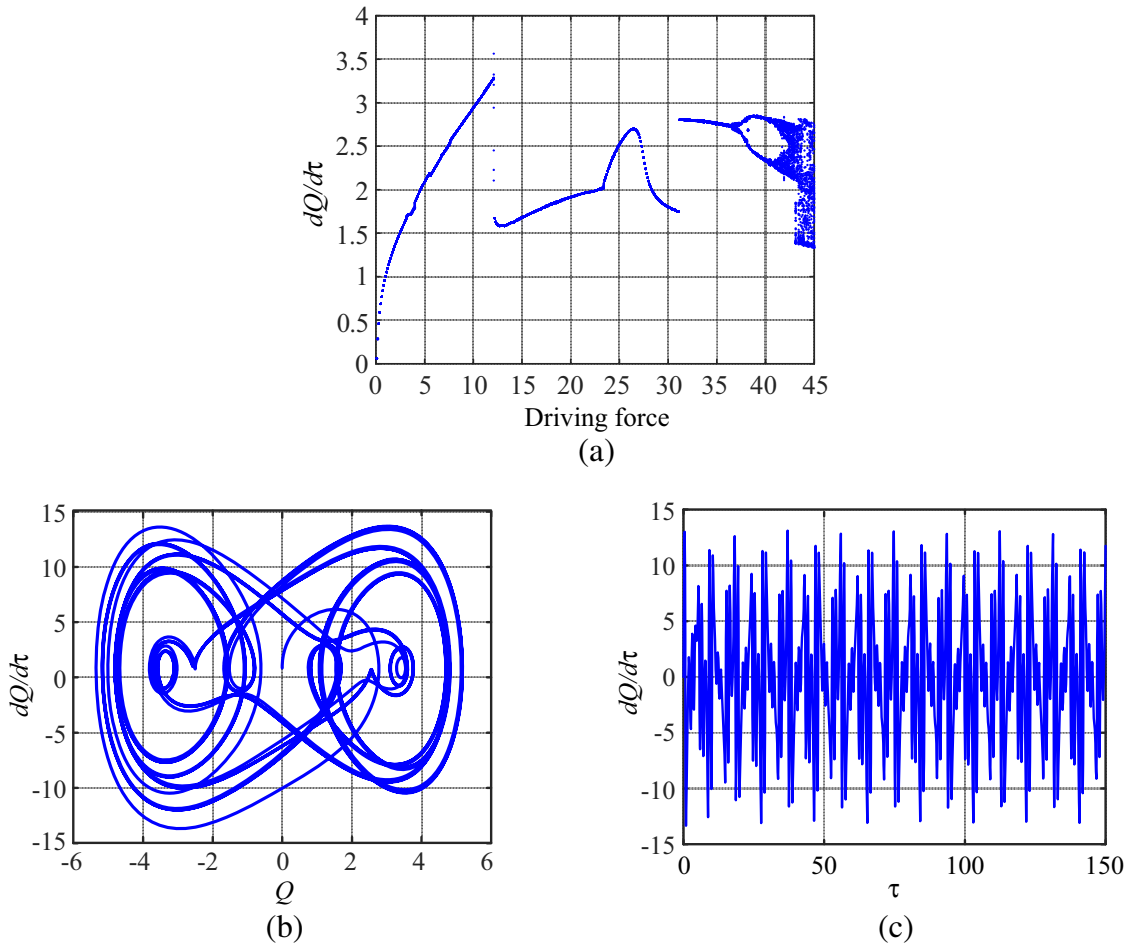

Figure 5. Nonlinear characteristics of the nonlinear MC-WPT system. (a) Bifurcation diagram. (b) The phase diagram at the driving force of 50. (c) The transient response at the driving force of 50.

when the driving force is in the range of [0, 40]. As shown in Fig. 4, the periodic state mainly consists of the periodic sinusoidal state and periodic non-sinusoidal state.

From the above analysis, it can be found that the state of the nonlinear system varies with the increase of the driving force. Generally, the MC-WPT system is operated in the periodic sinusoidal state which covers a small range of driving force. For efficient power delivery in a wider range of driving force, how the nonlinear MC-WPT system operated in the periodic non-sinusoidal state can be made use of is studied in this work. In the simulation, the driving force is set as 2.5. The frequency spectrum of Fig. 4(d) is depicted in Fig. 6(a). It can be seen that the periodic non-sinusoidal state is caused by high-order harmonics. To eliminate the high-order harmonics, an LC Chebyshev filter based waveform correcting circuit is designed. According to the design principle of the Chebyshev filter [36], the number and value of the inductors and capacitors are determined by advanced design system (ADS) software. The inductors and capacitors are connected by a π-type structure. For the nonlinear MC-WPT system operated in the periodic non-sinusoidal state, the waveform correcting circuit is shown in Fig. 6(b) where L_{f1}, L_{f2}, C_{f1}, C_{f2}, and C_{f3} are inductance and capacitance, respectively.

Figure 7 shows the waveform of $\frac{dQ}{d\tau}$ after adding the waveform correcting circuit. Comparing Fig. 7 with Fig. 4(d), the system state varies from the non-sinusoidal state to sinusoidal periodic state. It can be found that the waveform correcting circuit is efficient in eliminating high-order harmonics. With the waveform correcting circuit added, the restriction of the driving force on the nonlinear MC-WPT system is eliminated, and the system can be operated in a much wider range.

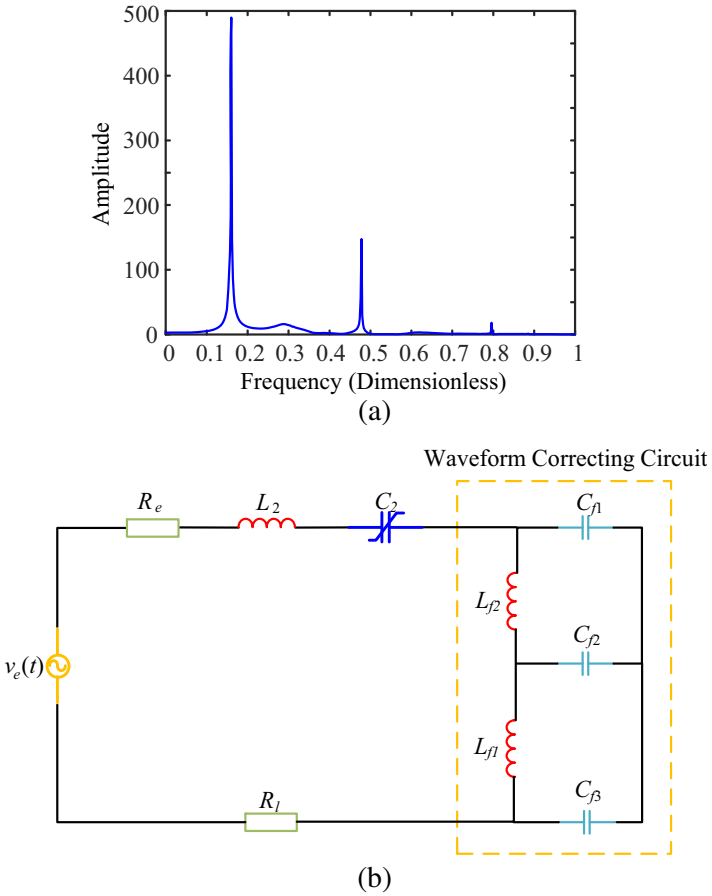

Figure 6. Frequency spectrum for the nonlinear MC-WPT system operated in the periodic non-sinusoidal state and the schematic diagram with the waveform correcting circuit. (a) Frequency spectrum. (b) Schematic diagram.

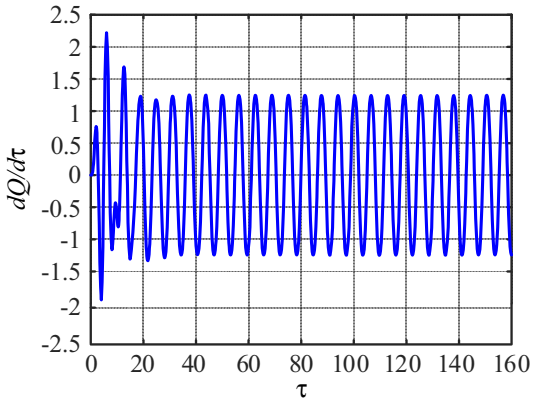

Figure 7. The transient response diagram with the waveform correcting circuit added.

4. EXPERIMENTAL VERIFICATION

In this section, a nonlinear MC-WPT system with a waveform correcting circuit is established, and its performance in the periodic non-sinusoidal state is examined. The experimental setup is shown in Fig. 8. A pair of anti-series connected varactor diodes (SMV1249) acts as a nonlinear capacitor in the

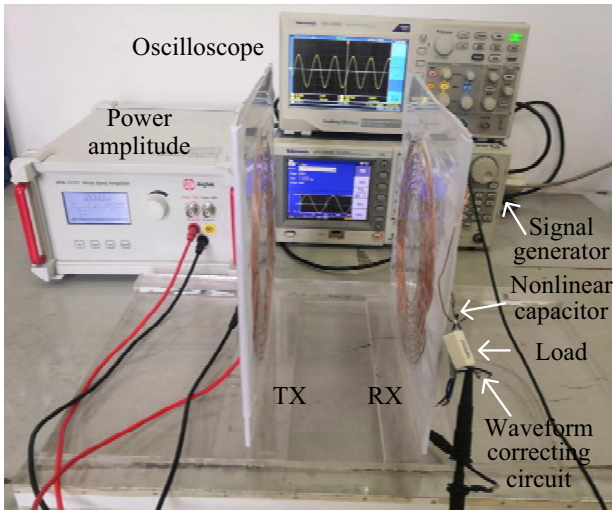

Figure 8. Experimental setup of the nonlinear MC-WPT system.

receiver. Both of the transmitting coil and receiving coil are wounded with copper wire whose diameter is 1.1 mm. For the two coils, the outer radius is 105 mm, and the inner radius is 45 mm. Besides, the number of turns is 11, and the distance between turns is 5 mm. At the transmitting side, the transmitter is connected with a signal generator via a power amplifier. At the receiving side, the receiver is linked to the waveform correcting circuit and then connected to the load. According to the measured inductance of the transmitter coil, the compensated capacitance at the resonant frequency of 1.25 MHz is calculated. The design specification of the system is summarized in Table 1.

Table 1. Design specification.

Component	Specification
Wire diameter	1.1 mm
Outer radius	105 mm
Inner radius	45 mm
Distance between turn	5 mm
Number of Turns	11 turns
Transmitting coil (L_1)	21.8 μH
Receiving coil (L_2)	20.5 μH
Primary capacitor (C_1)	810 pF
Load Resistance (R_L)	50 Ω
Nonlinear capacitance	Anti-series connected varactor diodes (SMV1249)
Waveform correcting circuit	$L_{f1} = 14.7$ nH, $L_{f2} = 14.7$ nH, $C_{f1} = 2.24$ nF, $C_{f2} = 7.27$ nF, $C_{f3} = 2.25$ nF

In Section 2, it has been revealed that the variation of driving force is determined by the powering excitation amplitude once the mutual inductance is fixed. In the experiment, the distance between coils is fixed. To validate the performance of the waveform correcting circuit, the excitation amplitude of the power is adjusted to make the system operate in periodic non-sinusoidal state. Fig. 9 compares the measured voltage across the load. In Fig. 9(a), the voltage is shown when the waveform correcting circuit is not added. It can be observed that the system is operated in the periodic non-sinusoidal state. Fig. 9(b) shows that the voltage when the waveform correcting circuit is added. Comparing Fig. 9(b) with Fig. 9(a), it can be found that the system is able to operate in periodic sinusoidal state with the

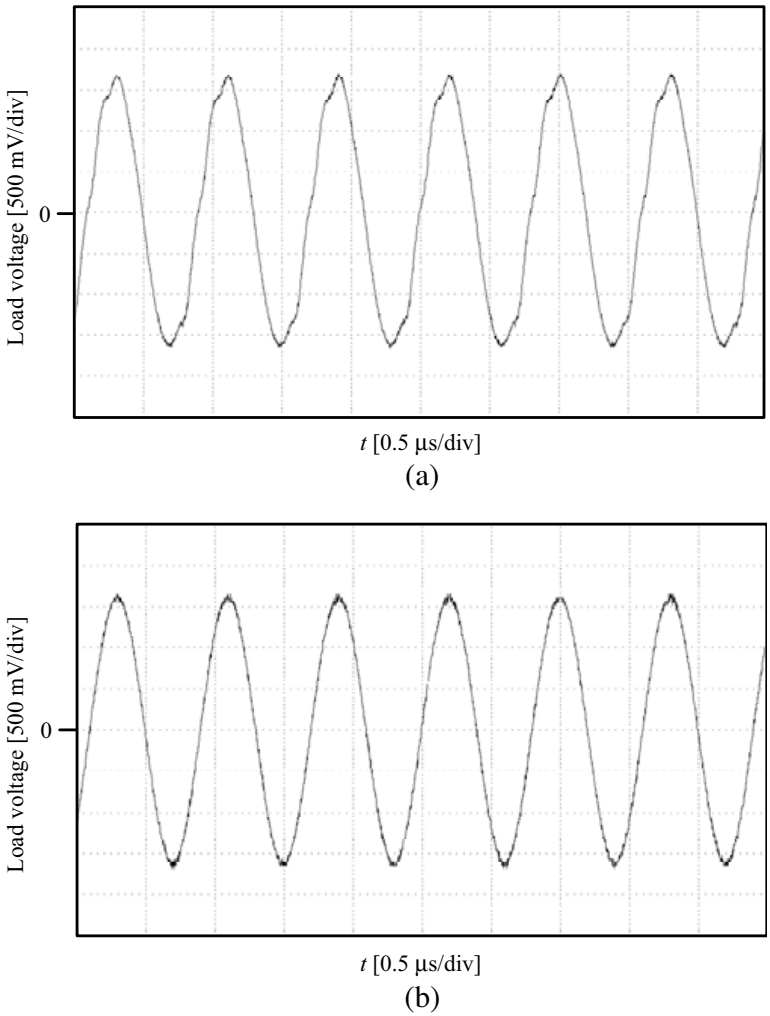

Figure 9. The transient response of the voltage across the load. (a) Without the waveform correcting circuit. (b) With the waveform correcting circuit.

waveform correcting circuit added. It should be noticed that the waveform correcting circuit is not required for the periodic sinusoidal state.

5. CONCLUSION

In this paper, a nonlinear MC-WPT system based on Duffing resonance is studied. The associated circuit model and mathematical model are established. It is found that the driving force has a direct impact on the performance of the MC-WPT system. Then the effect of the driving force is studied by simulation work. The result shows that the jump behavior occurs at the driving force of 1.6. To further evaluate the nonlinear characteristics, the phase locus and transient response of the system are investigated. It can be observed that the system is operated in periodic sinusoidal state when the driving force is much smaller than 1.6. Besides, the system is operated in periodic non-sinusoidal state when the driving force is larger than 1.6. However, once the driving force is too large, chaotic state is observed from the bifurcation diagram, and it should be avoided. For efficient power delivery in a wider range of driving force, the additional waveform correcting circuit is designed for the system operated in the periodic non-sinusoidal state. The results show that the nonlinear MC-WPT system can be operated in a wider range of driving force with the waveform correcting circuit added. Additionally, the robustness to frequency variation is generally kept.

ACKNOWLEDGMENT

This work was supported in part by the National Natural Science Foundation of China under Grants U1904182 and 61801172, in part by the Foundation for University Key Young Teacher by Henan Province of China under Grants 2020GGJS061, in part by the Natural Science Foundation of Henan Province of China under grant 212300410055, in part by the Science and Technology Project of Henan Province of China under grant 212102210012, and in part by the Scientific and Technological Innovation Program for Universities in Henan Province of China under Grant 21HASTIT018.

REFERENCES

1. Biswal, S. S., D. P. Kar, and S. Bhuyan, "Parameter trade-off between electric load, quality factor and coupling coefficient for performance enrichment of wireless power transfer system," *Progress In Electromagnetics Research M*, Vol. 91, 49–58, 2020.
2. Huang, Y. C., C. H. Liu, Y. Xiao, and S. Y. Liu, "Separate power allocation and control method based on multiple power channels for wireless power transfer," *IEEE Trans. Power Electron.*, Vol. 35, No. 9, 9046–9056, 2020.
3. Wang, M., J. Feng, Y. Fan, M. Shen, J. Liang, and Y. Shi, "A novel planar wireless power transfer system with distance-insensitive characteristics," *Progress In Electromagnetics Research Letters*, Vol. 76, 13–19, 2018.
4. Sahany, S., S. S. Biawal, D. P. Kar, P. K. Sahoo, and S. Bhuyan, "Impact of functioning parameters on the wireless power transfer system used for electric vehicle charging," *Progress In Electromagnetics Research*, Vol. 79, 187–197, 2019.
5. Wang, Q., W. Che, M. Dionigi, F. Mastri, M. Mongiardo, and G. Monti, "Gains maximization via impedance matching networks for wireless power transfer," *Progress In Electromagnetics Research*, Vol. 164, 135–153, 2019.
6. Parise, M. and G. Antonini, "On the inductive coupling between two parallel thin-wire circular loop antennas," *IEEE Trans. Electromagn. Compat.*, Vol. 60, No. 6, 1865–1872, 2018.
7. Parise, M., L. Lombardi, F. Ferranti, and G. Antonini, "Magnetic coupling between coplanar filamentary coil antennas with uniform current," *IEEE Trans. Electromagn. Compat.*, Vol. 62, No. 2, 622–626, 2020.
8. Shinohara, N., "The wireless power transmission: Inductive coupling, radio wave, and resonance coupling," *Wiley Interdisciplinary Rev.: Energy Environ.*, Vol. 1, No. 3, 337–346, 2012.
9. Ren, J. S., P. Hu, D. S. Yang, and D. Liu, "Tuning of mid-range wireless power transfer system based on delay-iteration method," *IET Power Electronics*, Vol. 9, No. 8, 1563–1570, 2016.
10. Jiwariyavej, V., T. Imura, and Y. Hori, "Coupling coefficients estimation of wireless power transfer system via magnetic resonance coupling using information from either side of the system," *IEEE J. Emerging Sel. Topics Power Electron.*, Vol. 3, No. 1, 191–200, 2015.
11. Casanova, J. J., Z. N. Low, and J. Lin, "A loosely coupled planar wireless power system for multiple receivers," *IEEE Trans. Ind. Electron.*, Vol. 56, No. 8, 3060–3068, 2009.
12. Ye, Z. H., Y. Sun, X. Dai, C. S. Tang, Z. H. Wang, and Y. G. Su, "Energy efficiency analysis of U-coil wireless power transfer system," *IEEE Trans. Power Electron.*, Vol. 31, No. 7, 4809–4817, 2017.
13. Costanzo, A., et al., "Conditions for a load-independent operating regime in resonant inductive WPT," *IEEE Trans. Microw. Theory Techn.*, Vol. 65, No. 4, 1066–1076, 2017.
14. Hui, S. Y. R., W. X. Zhong, and C. K. Lee, "A critical review of recent progress in mid-range wireless power transfer," *IEEE Trans. Power Electron.*, Vol. 29, No. 9, 4500–4511, 2014.
15. Shin, J., S. Shin, Y. Kim, S. Ahn, S. Lee, G. Jung, S. J. Jeon, and D. H. Cho, "Design and implementation of shaped magnetic-resonance-based wireless power transfer system for roadway-powered moving electric vehicles," *IEEE Trans. Ind. Electron.*, Vol. 61, No. 3, 1179–1192, 2014.
16. Nguyen, D. H., "Electric vehicle — Wireless charging-discharging lane decentralized peer-to-peer energy trading," *IEEE Access*, Vol. 8, 179616–179625, 2020.

17. Huang, L. Y., A. Murray, and B. W. Flynn, "A high-efficiency low-power rectifier for wireless power transfer systems of deep micro-implants," *IEEE Access*, Vol. 8, 204057–204067, 2020.
18. Huang, L. Y., A. Murray, and B. W. Flynn, "Optimal design of a 3-coil wireless power transfer system for deep micro-implants," *IEEE Access*, Vol. 8, 193183–193201, 2020.
19. Riehl, P., et al., "Wireless power systems for mobile devices supporting inductive and resonant operating modes," *IEEE Trans. Microw. Theory Tech.*, Vol. 63, No. 3, 780–790, Mar. 2015.
20. Zhang, Y. M. and Z. M. Zhao, "Frequency splitting analysis of two-coil resonant wireless power transfer," *IEEE Antennas Wireless Propag. Lett.*, Vol. 13, 400–402, 2014.
21. De Miranda, C. M. and S. F. Pichorim, "A self-resonant two-coil wireless power transfer system using open bifilar coils," *IEEE Trans. Circuits Syst., II, Exp. Briefs*, Vol. 64, No. 6, 615–619, 2017.
22. Wang, S. M., Z. Y. Hu, C. C. Rong, X. Tao, C. H. Lu, J. F. Chen, and M. H. Liu, "Optimisation analysis of coil configuration and circuit model for asymmetric wireless power transfer system," *IEEE Antennas Wireless Propag. Lett.*, Vol. 12, No. 7, 1132–1139, 2018.
23. Zhong, W. and S. Y. R. Hui, "Maximum energy efficiency operation of series-series resonant wireless power transfer systems using on-off keying modulation," *IEEE Trans. Power Electron.*, Vol. 33, No. 4, 3595–3603, 2018.
24. Lyu, Y. L., F. Y. Meng, G. H. Yang, B. J. Che, Q. Wu, L. Sun, D. Erni, and J. L. W. Li, "A method of using nonidentical resonant coils for frequency splitting elimination in wireless power transfer," *IEEE Trans. Power Electron.*, Vol. 30, No. 11, 6097–6107, 2015.
25. Lim, Y., H. Tang, S. Lim, and J. Park, "An adaptive impedance-matching network based on a novel capacitor matrix for wireless power transfer," *IEEE Trans. Power Electron.*, Vol. 29, No. 8, 4403–4413, 2014.
26. Wang, M., J. Feng, Y. Y. Shi, and M. H. Shen, "Demagnetization weakening and magnetic field concentration with ferrite core characterization for efficient wireless power transfer," *IEEE Trans. Ind. Electron.*, Vol. 66, No. 3, 1842–1851, 2019.
27. Ricketts, D. S., M. Chabalko, and A. Hillenius, "Tri-loop impedance and frequency matching with high-Q resonators in wireless power transfer," *IEEE Antennas Wireless Propag. Lett.*, Vol. 13, 341–344, 2014.
28. Stein, A. L. F., P. A. Kyaw, and C. R. Sullivan, "Wireless power transfer utilizing a high-Q self-resonant structure," *IEEE Trans. Power Electron.*, Vol. 34, No. 7, 6722–6735, 2019.
29. Wang, M., C. Zhou, M. H. Shen, and Y. Y. Shi, "Frequency drift insensitive broadband wireless power transfer system," *AEU-Int. J. Electron. Commun.*, Vol. 117, 2020.
30. Chen, Y. F., W. X. Xiao, Z. P. Guan, B. Zhang, D. Y. Qiu, and M. Y. Wu, "Nonlinear modeling and harmonic analysis of magnetic resonant WPT system based on equivalent small parameter method," *IEEE Trans. Ind. Electron.*, Vol. 66, No. 8, 6604–6612, 2019.
31. Assawaworrarit, S., X. F. Yu, and S. H. Fan, "Robust wireless power transfer using a nonlinear parity-time-symmetric circuit," *Nature*, Vol. 546, No. 7658, 387–390, 2017.
32. Abdelatty, O., X. Y. Wang, and A. Mortazawi, "Position-insensitive wireless power transfer based on nonlinear resonant circuits," *IEEE Trans. Microw. Theory Techn.*, Vol. 67, No. 9, 3844–3855, 2019.
33. Kovacic, I. and M. J. Brennan, *The Duffing Equation: Nonlinear Oscillators and Their Behavior*, Wiley, Hoboken, NJ, USA, 2011.
34. Wang, X. Y. and A. Mortazawi, "Bandwidth enhancement of RF resonators using duffing nonlinear resonance for wireless power applications," *IEEE Trans. Microw. Theory Techn.*, Vol. 64, No. 11, 3695–3702, 2016.
35. Vernizzi, G. J., S. Lenci, and G. R. Franzini, "A detailed study of the parametric excitation of a vertical heavy rod using the method of multiple scales," *Meccanica*, Vol. 55, No. 12, 2423–2437, 2020.
36. Gargour, C. S. and V. Ramachandran, "A simple design method for transitional Butterworth-Chebyshev filters," *J. Instit. Electron. Radio Eng.*, Vol. 58, No. 6, 291–294, 1988.